Applied Water Science (2020) 10:32
https://doi.org/10.1007/s13201-019-1114-6

ORIGINAL ARTICLE

Sequestered capture and desorption of hexavalent chromium from solution and textile wastewater onto low cost *Heinsia crinita* seed coat biomass

Folasegun A. Dawodu[1] · Benjamin M. Akpan[1] · Kovo G. Akpomie[2]

Received: 20 May 2019 / Accepted: 6 December 2019 / Published online: 19 December 2019
© The Author(s) 2019

Abstract

Due to the high cost associated with the treatment of effluents containing heavy metals in the environment, the continuous untreated release of effluent containing chromium from textile industries has resulted in several adverse effects to plants, ecological systems and humans. This research therefore focused on the use of a low cost, biodegradable *Heinsia crinita* seed coat (HCSC) material for the biosorption of chromium(VI) from aqueous and textile contaminated effluent. The biosorbent was characterized for specific surface area, surface morphology, pH point of zero charge and surface functional groups. Operational variables influences such as biosorbent dose, pH, temperature, initial Cr(VI) ion concentration and contact time on biosorption process was tested. The optimum biosorption parameter was obtained at pH 2.0, adsorbent dosage 0.25 g and contact time of 30 min. From sorption analysis, the pseudo-second-order model best described the attenuation kinetics. Concerning biosorption equilibrium, the results suggested that the adsorption isotherm obeyed the Freundlich model. Langmuir maximum monolayer biosorption capacity of 231.7 mg/g was higher than most biosorbents for Cr(VI) ion. The thermodynamic data showed a physical, spontaneous and endothermic biosorption process. HCSC showed high percentage desorption > 90% using 0.1 M HNO_3 and was efficient after three cycles of regeneration studies. The results showed HCSC biomass as a suitable candidate for abstraction of Cr(VI) ion from contaminated solution and textile effluent.

Keywords Biosorption · *Heinsia crinita* · Heavy metals · Kinetics · Effluent · Thermodynamics · Desorption

Introduction

One of the major hazards in the twenty-first century is environmental pollution, due to man's desire for improved yield in agriculture, technology and socioeconomic development with the use of chemicals. The mismanagement, improper treatment and discharge of chemically induced wastewater into the environment and its attendant effect on humans and living organisms are worrisome. Discharge of effluents emanated from various industries constitutes a large amount of physicochemical parameter that comprises nitrite, conductivity, nitrate, alkalinity, temperature, pH, oxygen demand, hardness, total suspended solid, phosphate, sulfate, organic, inorganic pollutants and heavy metal ions (Ibigbami et al. 2016). Some of these compounds have been validated to have a pronounced effect in most waste streams which include those emanating from industrial activities associated with breweries, battery manufacture and pharmaceuticals petrochemicals, distilleries, pulp and paper manufacture, petroleum production and blending of spirit, refining, metallurgical plants, fertilizer, pigment, paints, pesticide and herbicide industries, mining and tanneries as well as textiles industries (Asuquo et al. 2017). Among these industries, textiles are one of the leading consumers of water and complex chemicals during different stages of textile processing.

Heavy metals are gaining popularity in the list of pollutants that distort our environment because of their bioaccumulation and bio-concentration in living tissue, which further biomagnifies as they progress through the food chain (Sridhara et al. 2008). Heavy metals cannot be biodegraded or destroyed. Some of them are carcinogenic, mutagenic, teratogenic, toxic, poisonous, oxidizing, reducing, flammable

✉ Benjamin M. Akpan
benakpan4@gmail.com

[1] Department of Chemistry (Industrial), University of Ibadan, Ibadan, Nigeria

[2] Department of Pure and Industrial Chemistry, University of Nigeria, Nsukka, Nigeria

and very reactive, and they enter our body system through water, food, air and drinking. Effluents from textile mills also contain chromium which is one of the most toxic heavy metal, widely utilized by different industries (Al-Othman et al. 2012; Li et al. 2012). The existence of chromium in the environment is represented by the +3 and +6 oxidation state (Karimi et al. 2012). Chromium in the oxidation state of VI is more poisonous and harmful to human health than chromium in the oxidation of III (Samani et al. 2010). Chromium(III) exists in nature and is needed by the body to utilize fat, protein and sugar. The required dosage of Cr(III) for adults is 50–200 mg per day (Lazaridis and Asouhidou 2003). Contrarily, Cr(VI) barely exists in nature, but is normally discharged into the environment through human activities. It has been investigated and validated by the International Agency for Research on Cancer (IARC) that chromium(VI) is a potent carcinogen to humans. According to Environmental Protection Agency (EPA), the highest permissible amount of total chromium discharge into potable drinking water is 0.05 mg/L inland and in surface waters is 0.1 mg/L (EPA 1990). Consequent upon these, it is necessary and expedient to inhibit these metallic contaminants from polluting surface and ground water by condensation, dispersion, sedimentation, precipitation or dissolution and also to eliminate or lower their presence in order to reduce the likelihood of animal, plant and human uptake and eventual accumulation in the food chain (Mclaughlin et al. 2000; Kabata-Pendias 2001).

To recover and restore the heavy metal contaminated effluent, different currently developed treatment technologies were investigated by several researchers for remediation of wastewater soiled with heavy metals. The method reported includes membrane, separation, coagulation, ozonation, precipitation, ion exchange, solvent extraction and flocculation. All these methods possess characteristic limitations, such as high cost, and high-energy requirements (Padmesh et al. 2006). The quest for cheap and inexpensive technologies that involve abstraction of harmful metals from effluent has shifted to biosorption, according to sorbate–sorbent interaction. Different bio-adsorbents were used and showed significant biosorption uptake capacity for heavy metals from contaminated solution. Some of them include tamarind hull, rice straw, sawdust, rice husk, sunflower stem, sea-weed, wood, tea-waste, maize-corn cob, sugarcane bagasse, blue algae, Bael fruit, *Macadamia* nutshell, Cranberry kernel shell, rosehip seed shells, banana peel, etc. (Chojnacka et al. 2005; Anandkumar and Mandal 2009; Zahra et al. 2013; Pakade et al. 2017; Parlayici and Pehlivan 2019). The quest for the use of biosorbents with possibly higher adsorption potentials is necessary and ongoing. Out of these arrays of adsorbents, the seed coat of powdered *Heinsia crinita* which is readily available in Nigeria has not been utilized for the adsorption and successive desorption of Cr(VI) ion from polluted solution. *Heinsia crinita* belongs to the family of *Rubiaceae*, and it is locally known as Atama leaves (Okokon et al. 2009). It is a shrub with woody stem and branches and it is native to West Africa, particularly the southern part of Nigeria (Akinfolarin and Gbarakoro 2016). It is an evergreen scrambling shrub in secondary jungle, or small tree that averages 8–13 m in height. The leaves extract have been reportedly used in the treatment of skin rashes and the leaves for umbilical hernia. The leaf juice is also used in the management of various other gastrointestinal disorders (Etukudo 2003).

A thorough literature search revealed lack of information on bio-adsorbent prepared from *Heinsia crinita* seed coat for the abstraction of Cr(VI) ions or any other pollutant from aqueous solution and textile effluent. The objective of the study was to look at the potential biosorbent property of *Heinsia crinita* seed coat powder for remediating Cr(VI) ion and its desorption potential. The adsorbents effectiveness for removal of Cr(VI) from a contaminated textile effluent was also evaluated.

Materials and methods

Adsorbate preparation

Analytically reagent grade chemicals were used in this study without further purification. All the glasswares used were washed and rinsed several times. For preparation of stock solutions and dilutions, deionized water was used. Stock solution of 1000 mg/L Cr(VI) concentration was prepared by diluting 2.8288 g of Potassium dichromate in 1000 mL volumetric flask using deionized water. Serial dilution of stock solution was carried out to obtain solution of different concentration 100–500 mg/L. Adjustment of pH of the solution with 0.1 M NaOH and 0.1 M HNO_3 was done.

Biosorbent preparation

Heinsia crinita seed coat (HCSC) used as biosorbent in this study was obtained from a local farmland in Ikot Ekop, Akwa Ibom State, Nigeria. Thorough washing of the biomass with distilled–deionized water to discard impurities and adhered metal contaminants was done and was dried under the sun for 21 days. The seed coats were separated from the seed, washed with deionized water, and were later dried in air-supplied oven at 80 °C for 3 h. The resulted sample was thereafter milled into fine powder with the aid of a mechanical grinder (Thomas milling machine), and subsequently filtered in a sieve using 150 µm ASTM mesh size to obtain powders of uniform particle sizes. The biosorbent parts with particle diameter ≤ 150 µm were utilized.

Characterization

The functional groups present on HCSC were obtained using Fourier Transform Infrared spectrum (FT-IR) (Perkin Elmer FT-IR spectrophotometer, spectrum BX). Scanning electron microscopy (SEM) (JEOL JSM-5610LV, Japan) coupled with energy dispersive analysis of X-ray instrument (EDX) was used to determine the morphology. The pH of the slurry was obtained using a pH meter (Mettler Toledo). The pH drift method by prahas et al. (2008) was conducted to determine the pH_{pzc} of the adsorbent. Determination of bulk density was conducted using a 25 cm^3 density bottle. The specific surface area of HCSC was determined via Saers method (Saer 1956).

Wastewater was obtained from a textile industry located in Lagos state, Nigeria, and was characterized using standard methods as reported (FEPA 1991; APHA 2005; Skoog et al. 1998).

Batch biosorption test

Biosorption technique was carried out by equilibrating 0.25 g of HCSC with 50 mL of 200 mg/L Cr(VI) solution in a 250 mL stopper conical flasks for 120 min. The flask contents were agitated using a temperature-controlled mechanical shaker machine at 200 revolutions per minute at room temperature of 25 °C. The effect of pH was investigated at pH values of 2.0–8.0, HCSC dosage (0.05–0.30 g), contact time (0–180 min), initial Cr(VI) ion concentration (100–500 mg/L) and temperature (25, 40 and 55 °C). To study the effect of a parameter, the parameter was changed while maintaining others at the optimum conditions. As the given contact time for each experiment was exhausted, the mixtures were separated by filtration and centrifuged at 1500 rpm for 10 min thereafter 10 mL aliquots was taken. The filtrate was then analyzed using the Atomic Absorption Spectrophotometer (Buck Scientific Model 201VGP) (AAS). The percent metal uptake by the biomass and equilibrium adsorption amount q_e of HCSC biomass was calculated using Eqs. (1) and (2), respectively,

$$\%\text{Sorption} = \frac{C_o - C_e}{C_o} \times 100 \tag{1}$$

$$q_e = \frac{v(C_o - C_e)}{m} \tag{2}$$

where q_e (mg/g) is amount of equilibrium adsorption, C_0 represents the concentration of initial metal ion (mg/L), C_e is the equilibrium concentration (mg/L), V is the solution volume (L), m represents the weight of biomass (g).

Desorption/regeneration experiment

Desorption characteristics of Cr(VI) ion from spent HCSC were studied using the solvent elution method. This was carried out using 0.1 M HNO_3 as stripping agent. 0.1 g of dried Cr(VI) loaded adsorbent was mixed with 50 ml of the stripping agent and agitated for 1 h then filtered and the eluted Cr(VI) concentration from the filtrate was determined by the AAS. The percentage desorption was calculated by the equation (Chukwuemeka-okorie et al. 2018):

$$\%\ \text{Desorption} = 100\left[C_D V_D\right]/q_{em} \tag{3}$$

where C_D (mg/L) is the Cr(VI) ion concentration in desorbed solution, V_D (L) is the desorbed solution volume, mass of HCSC is represented by m (g) which is used for desorption and q_e (mg/g) is the adsorption capacity of HCSC for Cr(VI) ion. Three cycles of adsorption/desorption were performed to obtain the reusability of the biosorbent. The desorption–adsorption were performed under the same conditions described for adsorption and desorption. At the end of each cycle, the adsorbents were washed with deionized water and oven dried.

Validation of model

Chi-square X^2 analysis was carried out to ascertain the isotherm with best description of biosorption of Cr(VI) onto HCSC powder. The equation below gives the mathematical statement for X^2 analysis (Viswanathan et al. 2009):

$$x^2 = \sum \frac{\left(q_e - q_{e,m}\right)^2}{q_{e,m}} \tag{4}$$

where q_{em}, is the capacity of equilibrium determined by model calculation (mg/g) and q_e represents the experimental data on the capacity of equilibrium (mg/g). If the data from the model are analogous to the experimental data, the value of X^2 will reduce, but if they contrast, the value of X^2 will increase. It is also important to use the nonlinear chi-square test to analyze the data set to validate the best-fit isotherm for the mathematical description of the biosorption system.

For the kinetic models, the squared sum of error (SSE) values estimated the best fit. For accurate estimation of q_t value, SSE should be smaller and r^2 should be higher for a good fit of model with experimental data.

$$\text{SSE} = \sum \frac{\left(q_{t,e} - q_{t,m}\right)^2}{q_{t,e}^2} \tag{5}$$

where $q_{t,e}$ and $q_{t,m}$ are the corresponding values that are determined from the kinetic models and the experimental

capacity of biosorption of metal ions (mg/g) at time t. The value of q_e, k_1, R^2 along with squared sum of error values for all the kinetic models are calculated using Microsoft excel add on software.

Results and discussion

Characterization of HCSC powder

Characterization of the biomass (Table 1) portrayed that HCSC powder contained moisture content, 3.36%; ash content, 0.83%, volatile matter, 27.51%; and fixed carbon, 68.30%. The results presented herein were obtained from the mean of duplicate determinations. The low moisture content helps in the preparation of the HCSC, since they require less drying before use. The existence of low moisture content confirms the presence of very low fatty content in HCSC (Kamsonlian et al. 2012). The carbon content fixed value of HCSC determined from proximate and ultimate analysis was 70.40% and 68.30%, respectively. The high carbon content of HCSC powder showed the potentials of HCSC as a good candidate for sequestering heavy metal ions from polluted wastewater. The bulk density of the HCSC powder was 0.38 g/cm^3. The analysis results also showed that the surface area, slurry pH, and average particle size of the biosorbent was 176.6 m^2/g, 4.57 and 75–150 µm, respectively. The pH_{zpc} is the value of pH with equal positive and negative charges on the surface of HCSC biomass. The pH_{zpc} of HCSC biomass was found to be 7.01. However, precipitation may account for metal removal at higher pH values above 6.0. Therefore, lower pH values were utilized in the sorption experiment to avoid precipitation of Cr ions in form of insoluble hydroxides.

Table 1 Physicochemical characterization parameters of HCSC

Parameter	Value
Moisture content (%)	3.36
Ash content (%)	0.83
Volatile matter (%)	27.51
Fixed carbon content (%)	68.30
pH_{ZPC}	4.12
Tapped bulk density (g/cm^3)	0.38
Slurry pH	4.57
SSA (m^2/g)	176.6
Average particle size (µm)	75–150 µm
Elements	% composition
Elemental composition of HCSC biomass	
Ag	0.14
Si	0.12
C	70.40
Mg	0.38
O	6.00
Cu	3.42
Al	18.69
Fe	2.78

The morphology and elemental composition of HCSC biomass was obtained by SEM and EDX analysis respectively (Fig. 1). It was observed that the surface of HCSC was irregular and heterogeneous. The existence of protrusions pores was not distributed evenly, but moved within the cell matrix of the biomass (Kamsonlian et al. 2012). The surface roughness of the biomass revealed the availability of a large surface area (176.6 m^2/g) of biosorbent for metal binding. The EDX analysis of HCSC powder was carried out to ascertain the composition of the element of the sample. Table 1 shows the results of the elemental analysis. The result (Fig. 1) also revealed sharp peaks for the elements C, O and Al, and smaller peaks for Cu, Ag, Fe, Mg and Si. The existence of Al, O and Si as well as Fe in the biosorbent further reveals the presence of aluminosilicate in the biomass. The high surface area, proximate and ultimate analysis results were comparable to those obtained by other researchers (Ahmad et al. 2017, Eze et al. 2019; Yusuff 2019) suggesting good potentials of HCSC as biosorbent for Cr(VI) ions.

The FT-IR spectrum of HCSC powder was recorded to obtain surface functional groups of sorption and is shown in Fig. 2. The FT-IR spectrum revealed that HCSC powder had several functional groups, which could be utilized for Cr(VI) sorption on the adsorbent. Peaks were observed at 3778 cm^{-1}, 3493 cm^{-1}, 3133 cm^{-1}, 2853 cm^{-1}, 2713 cm^{-1}, 2353 cm^{-1}, 1645 cm^{-1}, 1482 cm^{-1}, 1285 cm^{-1}, 1205 cm^{-1}, 949 cm^{-1}, 666 cm^{-1} and 373 cm^{-1}. The peaks at 3778–3133 cm^{-1} indicated the presence of (O–H stretch). The peaks at 2853 cm^{-1} were attributed to symmetric and asymmetric (C–H) stretching of aliphatic methylene and methyl (Yargic et al. 2014). Similarly, the peaks at 2713 cm^{-1} were indicative of symmetrical and asymmetrical stretch of alkanes, the presence of (C≡C) vibrations in the alkyne groups was attributed to 2353 cm^{-1}. The 1645 cm^{-1} peak corresponded to the existence of (−C = O) stretch of carbonyl moieties, 1482 cm^{-1} was attributed to the (C = C) ring stretch of aromatic compound. Furthermore, the peaks at 1285 and 1205 cm^{-1} were indicative of (C–N/C–O) stretch of ether. The peak at 949 cm^{-1} is indicative of the presence of (C–H) deformation of mono-substituted alkenes, 666 cm^{-1} indicated the existence of (C–H) bonding stretch (out of plane) of alkenes and the peaks at 373 cm^{-1} were assigned to the presence of aliphatic phosphorus compound. Furthermore, the occurrence of the peaks at 492.61 cm^{-1} and 400 cm^{-1} indicated the existence of Si–O–Si, Al–O–Si stretch, or C–C/C–H stretch of aromatic compound (Njoya

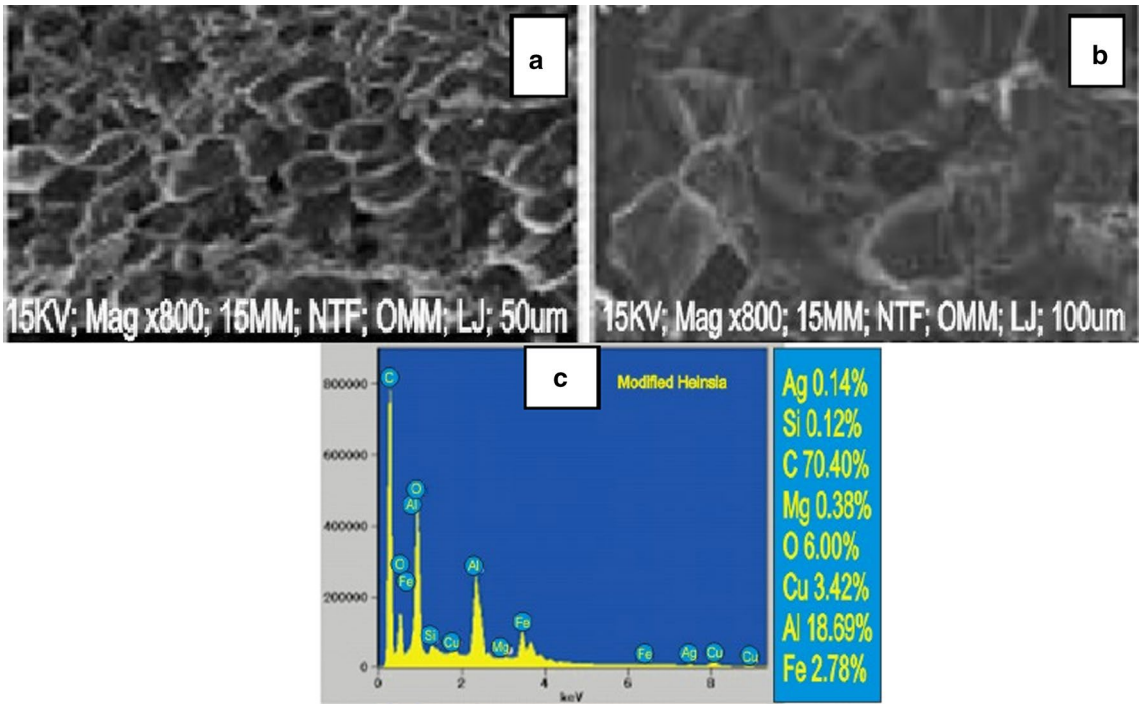

Fig. 1 SEM micrograph of unloaded HCSC powder surface at **a** 50 µm and **b** 100 µm, **c** EDX of the HCSC adsorbent

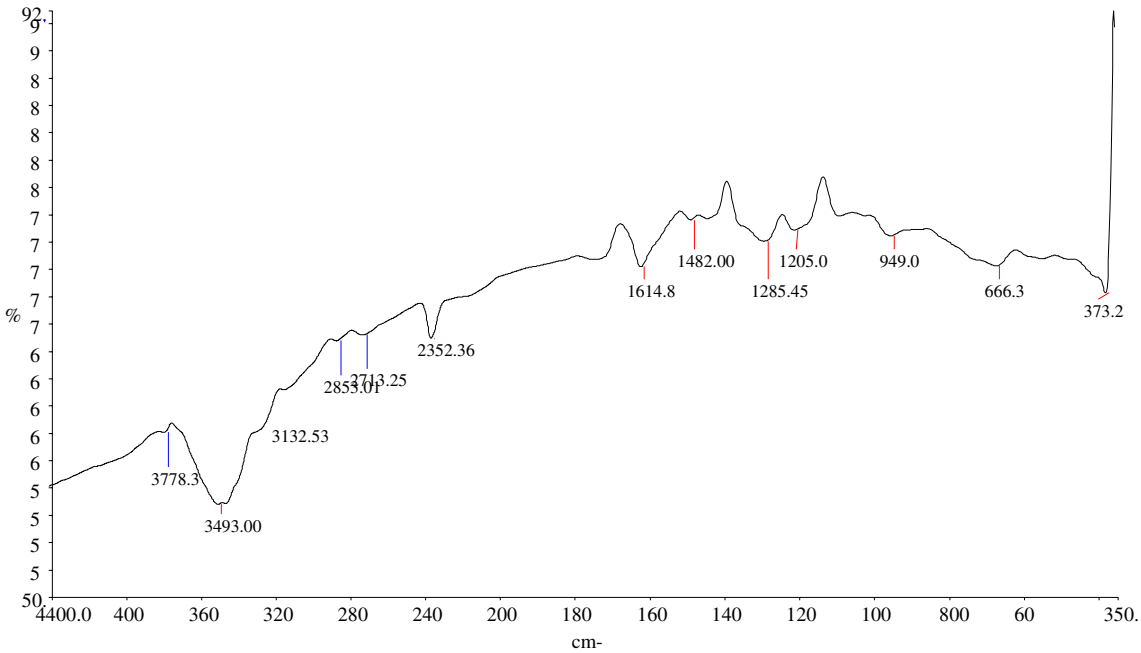

Fig. 2 Fourier transform infrared spectra of HCSC powder

et al. 2006). The existence of the Al–O–Si and Si–O–Si groups on the biomass surface may indicate the presence of silicon and aluminum compounds depicted in the EDX spectra of the adsorbent of HCSC.

Influence of pH on removal of Cr(VI)

The pH is a substantial variable that regulates the heavy metal abstraction from wastewater. Figure 3 gives the percent removal and biosorption capacity and of Cr(VI) as a

function of pH in the range of 2.0–8.0. It was shown from the result that the amount of Cr(VI) sorbed (mg/g) on HCSC powder reduced with rise in pH. Similarly, the extents of Cr(VI) removal by HCSC powder also showed a decrease with pH increase. The optimum amount (mg/g) of Cr(VI) on HCSC was 49.45 mg/g at pH 2 while the maximum percent removal of Cr(VI) was 98.90%. The possible explanation for this observation is that at reduced pH, Cr(VI) may occur as $Cr_2O_7^{2-}$or $HCrO_4^{2-}$ in solution and has the tendency to interact with protonated active sites of the biosorbent (Aksu et al. 2002) but as pH of the solution rises, the biomass surface becomes negatively charged due to less H^+ ions, which repel the negatively charged dichromate ions on the biomass surface, thereby affecting biosorption of Cr(VI). Different investigators have also profiled the dependence of pH of solution on metal ions biosorption (Anjana et al. 2007; Kiran et al. 2007). Consequent upon this, at pH 2.0, maximum adsorption was observed which made it the optimal pH suitable for subsequent studies. Several researchers have reported similar results on Cr(VI) removal from aqueous solutions using different biomasses like *Caryota urens* inflorescence waste (Rangabhashiyam and Selvaraju 2014), Tamarind wood (Acharya et al. 2009) and Bael fruit shell (*Aeglemarme loscorrea*) (Anandkumar and Mandal 2009).

Effects of biosorbent dose

The biosorbent dosage is an important parameter that must be investigated during the biosorption of metal ions. Figure 4 shows the adsorptive capacity of HCSC and the adsorbent dosage effect on the percentage removal of Cr(VI). The results show that the percentage removal and biosorption capacity of Cr(VI) increases as the adsorbent dosage increases. This increase occurred due to increase in the number of adsorption sites accessible for biosorption (Cardoso et al. 2011). Similar observation have been validated by Rafatullah et al. (2009) for Cu (II) removal by sawdust of sissoo tree (*Dalbergia sissoo*), *Caryota urens* inflorescence waste (Rangabhashiyam and Selvaraju 2014), and Tamarind wood (Acharya et al. 2009). On this basis, 0.25 g was chosen as the optimum dosage for sorption of Cr(VI) for further studies. The use of an amount greater than this did not give any significant advantage in the removal percentage of Cr(VI).

Effects of contact time

In the study of adsorption kinetics, the adsorption rate is very important. The effect of contact time was determined by checking the uptake of the metal ions in model solutions over a given period of 180 min at 25 °C. Figure 5 summarizes the result. The rate at which Cr(VI) was sorbed was very rapid during the initial contact but decreased gradually and reached equilibrium at 30 min. Thereafter no visible change in Cr(VI) removal was observed. The short contact time shows that HCSC biomass has the potential to abstract heavy metals from contaminated wastewater. The optimum adsorption capacity was achieved within 30 min. Further increase in contact time did not yield a positive result. The presence of additional vacant sites at the initial stage may have contributed to the initial rapid phase, as a result of the presence of high concentration gradient between sorbate in solution and sorbate on the adsorbent (Dawodu and Akpomie 2014). This observation can be explained based on the attraction between Cr(VI) molecules and the HCSC,

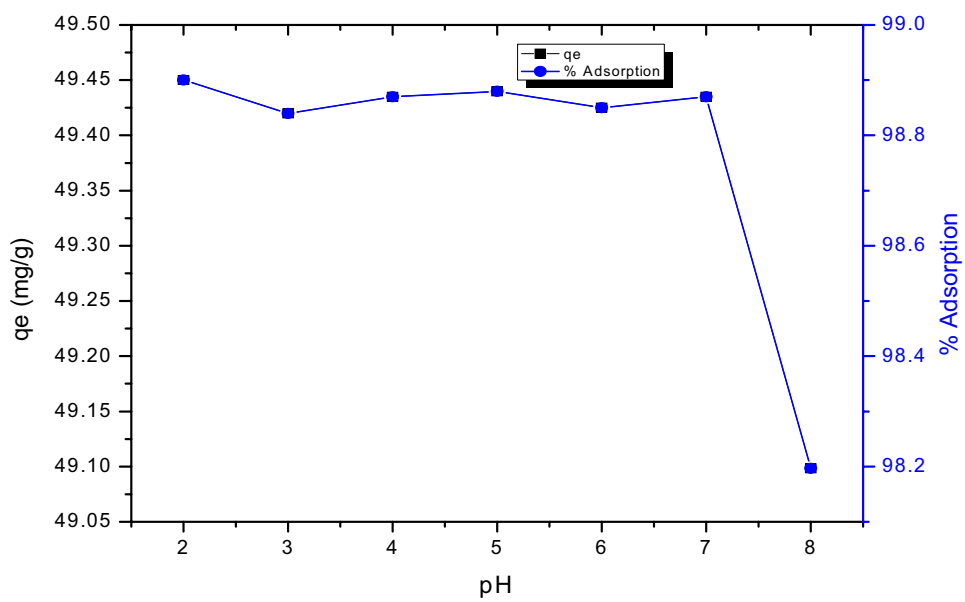

Fig. 3 Effect of pH on the biosorption of Cr(VI) on HCSC adsorbent

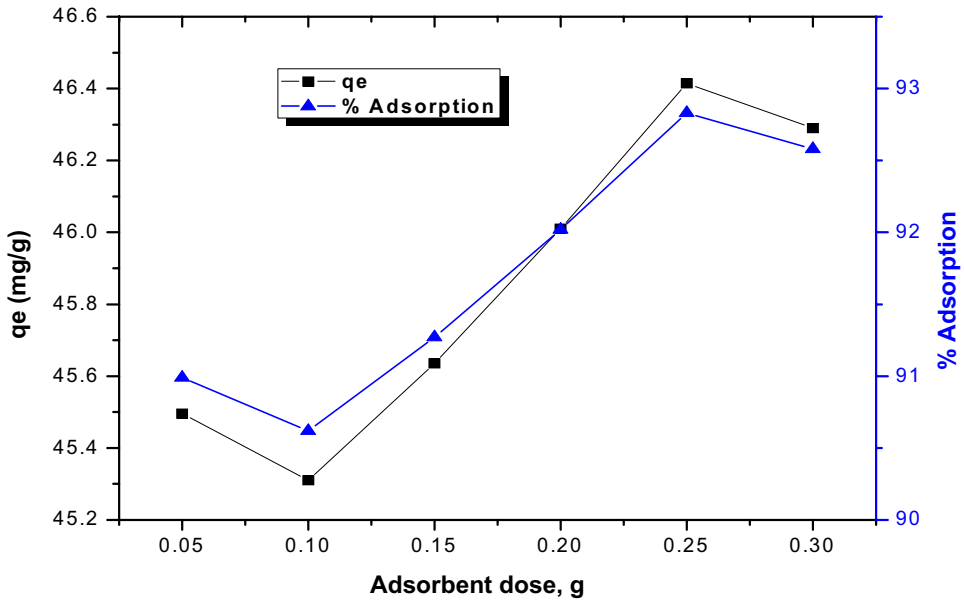

Fig. 4 Effect of adsorbent dosage on the biosorption of Cr(VI) ion on HCSC adsorbent

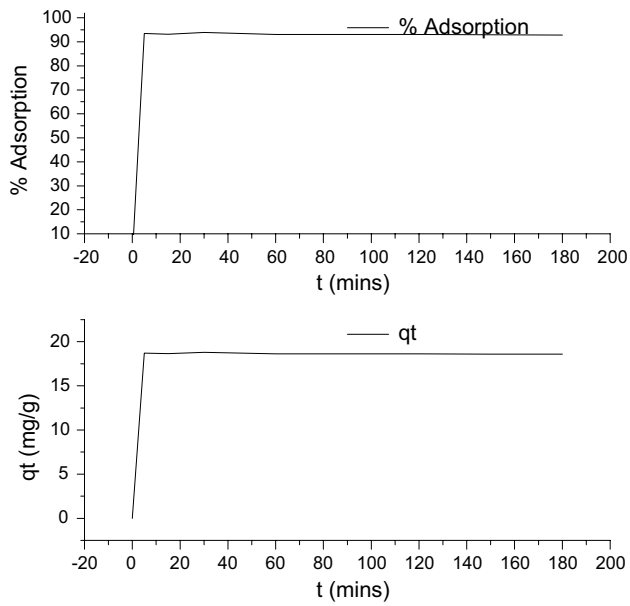

Fig. 5 Effect of contact time on the biosorption of Cr(VI) ion on HCSC adsorbent

secondly, by the fast diffusion of the Cr(VI) ions onto the surface and inter-particle matrix to attain rapid equilibrium.

Effect of Initial Cr(VI) concentration on HCSC biosorption

In the study of isotherms, the effect of initial concentration is vital. Determination of initial metal concentration was examined by changing the initial concentration from 100 to 500 mg/L and keeping all the other factors constant. The biosorption capacity of Cr(VI) onto HCSC is presented in Fig. 6. It was observed that an increase in the initial metal concentration from 100 to 500 mg/L, initially increased the biosorption biomass capacity with increasing initial concentration of metal ions. It was also observed that with increasing initial concentration of metal ions from 200 to 500 mg/L, the percentage removal Cr(VI) ion decreased. This decrease in adsorption is because of the fixed number of active sites of all the adsorbents and at higher concentrations, the active sites become saturated (Tsia and Chen 2010). Furthermore, an increase in concentration of initial metal ion with increase in the metal ions adsorption capacity was obtained. This observation is due to the elevated concentration gradient which serves as a driving force to overcome the resistance to mass transfer of the metal ions between the adsorbent and adsorbate species (Dawodu and Akpomie 2014). Similar findings has been reported by (Rangabhashiyam and Selvaraju 2014) and (Acharya et al. 2009) for hexavalent Cr(VI) removal from aqueous effluent. For subsequent sorption studies, 200 mg/L of Cr(VI), which gave an optimum percentage removal was used.

Effects of temperature

Temperature effect on the amount of Cr(VI) sorbed on HCSC powder and percentage removed was assessed at three different temperatures: 25, 40 and 55 °C. Figure 7 shows that metal ions adsorption on HCSC powder depends highly on the temperature. The maximum adsorption by HCSC was observed at 55 °C. The output indicates that the percentage removal of metal ions rose sharply with rise in temperature. This observation can be ascribed to

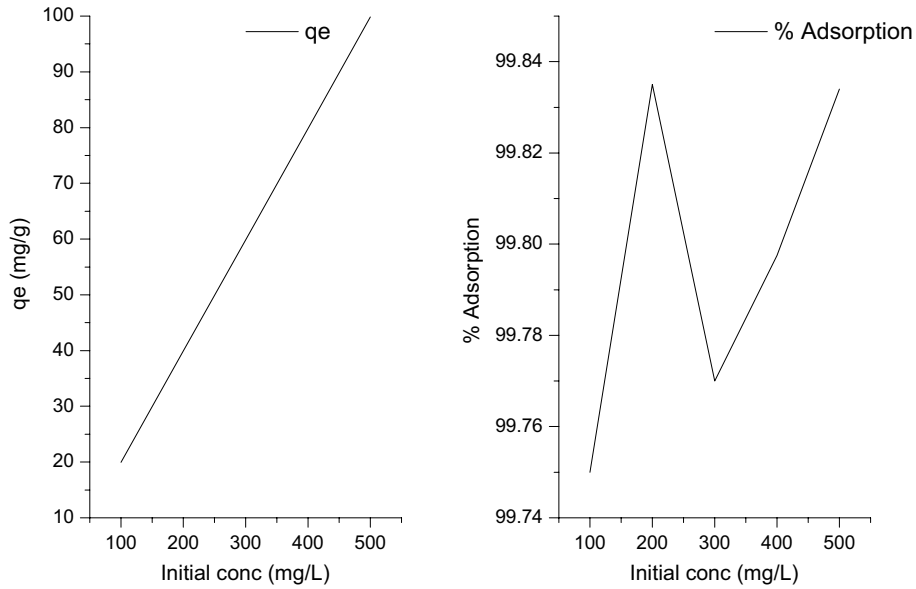

Fig. 6 Effect of initial metal ion concentration on the biosorption of Cr(VI) ion HCSC adsorbent

the increased HCSC pore size, swelling effect of HCSC, surface activation, and increase in movement of the Cr(VI) ion onto HCSC (Rangabhashiyam and Selvaraju 2014). Similar findings have been well documented in the literature on the removal of chromium(III), copper(II), lead(II) ions and nickel(II) from aqueous solutions by meranti sawdust (Rafatullah et al. 2009).

HCSC maximum adsorption capacity for Cr(VI) has been compared with other reported adsorbents in the literature as presented in Table 2. It revealed that HCSC recorded a higher adsorption than many of the adsorbents indicating the efficiency of this biosorbent.

Kinetic modelling

The study of kinetic modelling-based studies gives a better understanding of the reaction and mechanisms of the sorbate–sorbent interaction and helps to explain several specific parameters for monitoring and evaluating system performance. To differentiate kinetics equation based on solution concentration from solid adsorption capacities, the pseudo-first-order (PSO) equation was applied (Ho and Mckay 1998; Ani et al., 2019). The pseudo-first-order equation is expressed generally as follows:

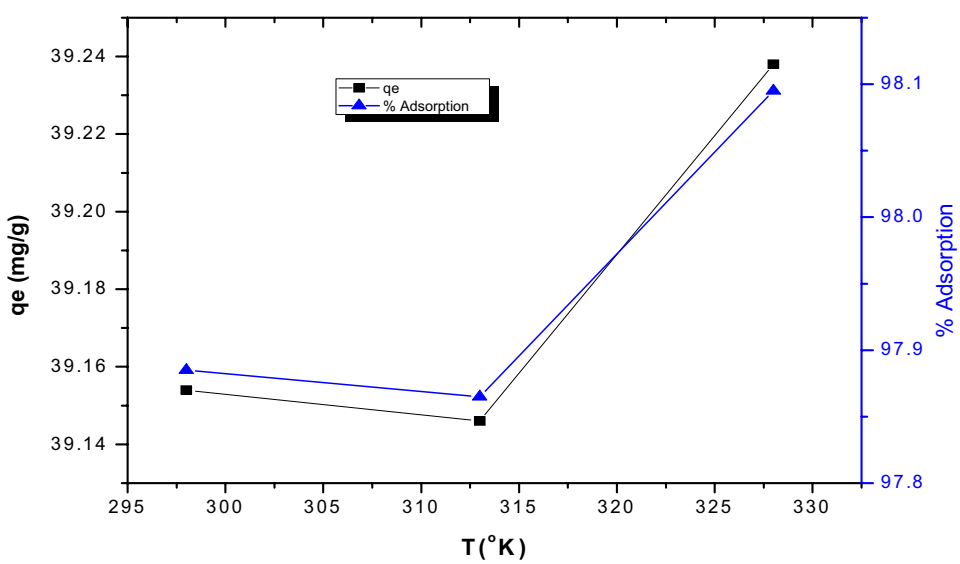

Fig. 7 Effect of solution temperature on the percentage removal and adsorption uptake capacity of Cr(VI) ions from solution unto HCSC

$$\log\left(q_e - q_t\right) = \log\left(q_e\right) - \frac{k_1 t}{2.303} \quad (6)$$

where q_t and q_e (mg/g) are the capacities of adsorption at time t (min) and equilibrium, respectively, and K_1 (min^{-1}), is the rate constant of the pseudo-first-order adsorption. The value of q_e, k_1,R^2 along with SSE values for the PFO model was calculated and summarized in Table 3. For the pseudo-first-order model, the $q_{e,\text{cal}}$ obtained for HCSC adsorbent was 0.8470 mg/ g and the value of the determination coefficient (r^2) and SSE obtained were 0.1505 and 7.6697. Based on the low and high values of r^2 and SSE, it can be inferred that the sorption process was not well described by the PFO model. It is seen from the table that the PFO equation gave the worst fit to the experimental result for Cr(VI) metal ions.

The PSO kinetic model of Ho and Mckay (1998) is expressed as:

$$\left(\frac{t}{q_t}\right) = \frac{1}{k_2 q_e^2} + \frac{1}{q_e}(t) \quad (7)$$

The initial adsorption rate constant h (mg/g min) is given as:

$$h = k_2 q_e^2 \quad (8)$$

where K_2 represents the rate constant of PSO adsorption (g/mg min),q_t is the amount of divalent metal ions on the adsorbent surface at any time, t (mg/g) and q_e the amount of divalent metal ions sorbed at equilibrium (mg/g). However, if the adsorption process obeys PSO model, then the plot of $\left(t/q_t\right)$ versus t will give a linear graph. The PSO model assessment of HCSC sorption kinetics of Cr(VI) ions is presented in Table 3. The PSO rate constant (k_2) was −0.33 $\text{g mg}^{-1}\ \text{min}^{-1}$. From this model, the rate of initial sorption (h) acquired from the pseudo-first-order model was −114.04 $\text{mg g}^{-1}\ \text{min}^{-1}$ and the metal ion loading values acquired from the pseudo-first-order model ($q_{e,\text{cal}}$) was 18.59 mg/ g. The values of r^2 and SSE are 1 and 0.000884. An assessment of the value of $q_{e,\text{cal}}$ and the error parameters from the two models compared to the experimental value $q_{e,\text{exp}}$ indicated that HCSC adsorbent uptake of Cr(VI) ion is best explained by the PSO model. It therefore showed that the PSO model (Kumar et al. 2010) more suitably explained the investigated system. The output obtained in this study for the kinetics of Cr(VI) ion is similar to what has been reported by investigators on the kinetics of metal sorption using *Caryotaurens inflorescence* waste biomass (Rangabhashiyam and Selvaraju 2014), for Cr(VI) removal from aqueous solutions, Cu(II) ions removal from aqueous effluents by blackgram bran (BGB) (Nadeem et al. 2009) and Cu(II) and Cd(II) ions biosorption by wheat straw (Dang et al. 2009). A comparative plot of experimental and calculated values of adsorption capacity q_t (mg/g) was plotted for Cr(VI) and is depicted in Fig. 8. It is evident that the experimental value for Cr(VI) sorption is well described by PSO model.

In intraparticle diffusion process, ions migrate into the inner pore spaces of adsorbent particles through different pore sizes.

Table 3 Kinetic parameters for the adsorption of Cr(VI) ion onto HCSC

Kinetic models	Cr(VI)
$q_{e,\text{exp}}$ (mg/g)	18.79
Pseudo-first order	
$q_e$cal (mg/ g)	0.8470
K_1 (min^{-1})	9.4423E−8
R^2	0.1505
SSE	7.6697
Pseudo-second order	
h ($\text{mg g}^{-1}\ \text{min}^{-1}$)	−114.04
$q_e$cal (mg/ g)	18.59
k_2 (g/ mg)	−0.33
R^2	1
SSE	0.000884
Intraparticle diffusion model	
K_{id}	0.7707
I	10.971
R^2	0.3348
SSE	3.3261

Table 2 Comparison of maximum monolayer adsorption capacity of adsorbents

Adsorbent	q_e (mg g^{-1})	References
Saw dust	15.84	Dakiky et al. (2002)
Olive cake	33.4	Dakiky et al. (2002)
Pine needles	21.5	Dakiky et al. (2002)
Brazilian-pine fruit wastes	240	Vaghetti et al. (2008)
Pinussylvestris (cone biomass)	201.81	Ucun et al. (2002)
Ocimum basilicum (mucilaginous seed)	205.0	Melo and Souza (2004)
Imidazole grafted silica	113.0	Li et al. (2007)
Lyngbyaputealis HH-15 (algae)	113.6	Kiran et al. (2007)
Heinsia crinita seed coat	231.7	This work

According to Weber and Morris (1963) to identify whether the sorption process is intraparticle diffusion mechanism or not, the intraparticle diffusion equation should be applied

$$q_t = k_{id} t^{1/2} + c \tag{9}$$

where k_{id} is the intraparticle rate constant (mg/g min$^{0.5}$) and C represents the intercept. If the sorption process is controlled by intraparticle diffusion, the plots of q_t versus $t^{0.5}$ will yield a straight line passing through the origin. Intraparticle diffusion model was applied to describe the adsorption mechanism of Cr(VI) ion onto HCSC. From Table 3, a very low regression r^2 of 0.3348 and high SSE of 3.3261 clearly indicated that intraparticle diffusion was not the rate-controlling mechanism of the adsorption process. The boundary layer effect was also described by the intercept of the plot C, which gave insight into the existence of the surface binding of the sorbate onto HCSC, thus indicating that intraparticle diffusion was not the rate-controlling mechanism (Dawodu and Akpomie 2014).

Biosorption isotherm modeling

Two parameter sorption isotherm models were utilized for fitting data in other to determine the relationship between the amount in aqueous concentration at equilibrium and the amount sorbed. In the current investigation, the Freundlich, Langmuir, Dubinin–Radushkevich (D–R) and the Temkin models were utilized (Chukwuemeka-okorie et al. 2018; Dawodu et al. 2019) to examine the equilibrium between the concentration in solution and the Cr(VI) ions sorbed onto HCSC biomass.

The Langmuir isotherm (Langmuir, 1918) can be represented as:

$$\frac{1}{q_e} = \frac{1}{Q_o} + \frac{1}{Q_o k_L C_e} \tag{10}$$

where Q_o is the maximum coverage capacity of the monolayer (mg/g) and K_L represents the Langmuir isotherm constant (L/mg). Langmuir isotherm is described by certain essential features expressed in terms of equilibrium parameter $R_{L,}$ which is a dimensionless constant also called separation factor (Webber and Chakravarti 1974).

$$R_L = \frac{1}{1 + k_L C_o} \tag{11}$$

R_L values describes the nature of adsorption to be either linear, if R_L=1, unfavorable if ($R_L > 1$), irreversible, if $R_L = 0$ and favorable if $0 < R_L < 1$ (Akpomie et al. 2019). The separation factor R_L (Fig. 9) showed a favorable biosorption of Cr(VI) on HCSC powder as R_L values were all within 0 and 1 (Hall et al. 1966). However, the low R^2 and high X^2 indicated that this model did not fit the biosorption data. This indicated that biosorption of Cr(VI) on HCSC cannot be attributed to a monolayer homogenous surface process.

Freundlich Isotherm model can be expressed by the equation (Ouyang et al. 2014):

$$\log Q_e = \log k_f + \frac{1}{n} \log C_e \tag{12}$$

where n is the intensity of adsorption and k_f is the Freundlich isotherm constant. This empirical equation speculates that the stronger binding site is occupied first and that degree of site occupation increases as the binding strength reduces

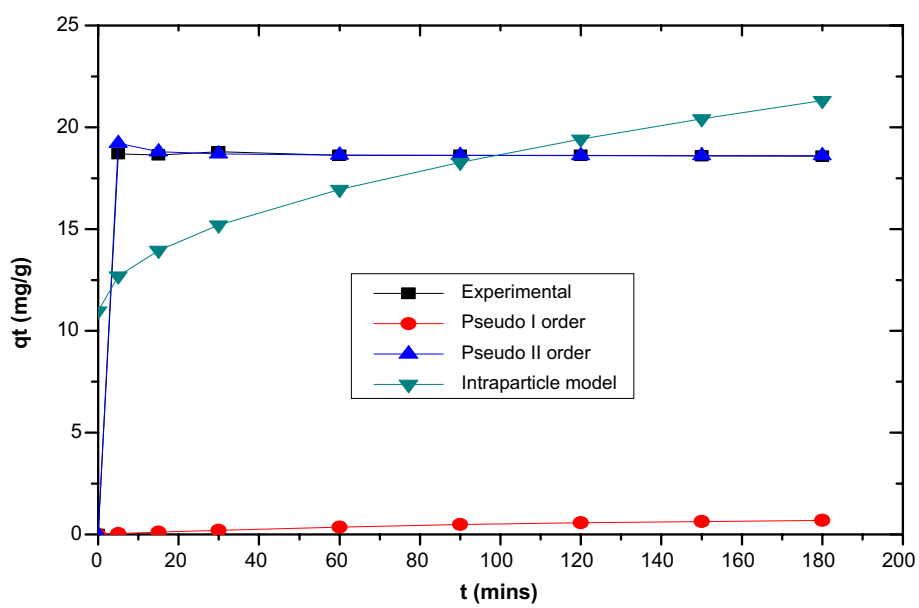

Fig. 8 Comparison of the experimental, pseudo-first-order, pseudo-second-order and intraparticule diffusion kinetic parameters for sorption of Cr(VI) on HCSC powder

(Padmesh et al. 2006). If value of $1/n$ is less than one, it indicates a normal adsorption and $1/n$ above one indicates cooperative adsorption. From Table 4, the value of $1/n$ was 1.09, which indicated a cooperative adsorption process between Cr(VI) and HCSC adsorbent surface. Similar $1/n$ value for Cr(VI) has been reported by Ozdemir et al. (2004) in the biosorption of cadmium(II), copper(II) and chromium(VI) by *Pantoea* sp. TEM18. On the basis of R^2, and x^2 value, the Freundlich model fits the adsorption isotherm data more than the Langmuir model (Table 4). The agreements between the experimental data and the Freundlich model-predicted value for metal ions sorption onto HCSC are portrayed in Fig. 10.

The Temkin isotherm model was applied in its linear form and is expressed as (Tempkin and Pyzhev 1940).

$$q_e = BInA_T + BInC_e \tag{13}$$

$$B = \frac{RT}{b_T} \tag{14}$$

where R is the universal gas constant (8.314 J/mol/k), b_T is the isotherm constant, A_T is the Temkin equilibrium binding constant (L/g) and, and T, temperature. Although the Temkin model presented the lowest χ^2 value and good fit to the biosorption, however, the R^2 of the Freundlich and D–R isotherm were better, showing the unfitness of this model to the biosorption as the Freundlich model, which also presented a relatively low χ^2.

Dubinin–Radushkevich isotherm model is expressed in its linear form as (Gunay et al. 2007; Dawodu et al. 2019).

$$\ln q_e = \ln q_s - K_{ad}\varepsilon^2 \tag{15}$$

Where q_s is the saturation capacity of the theoretical isotherm (mg/g) and K_{ad} = isotherm constant of Dubinin–Radushkevich (mol^2/kJ^2) and ε the Polanyi potential. The Dubinin–Radushkevich isotherm has been employed to differentiate between mean free energy of metal ions and its chemical and physical adsorption, E per molecule of adsorbate (Dubinin 1960). The D–R energy values give important information on the prediction of the nature of biosorption process, If 8 kJ/mol > E the biosorption process is controlled by physisorption and if E is between 8 and 16 kJ/mol its chemisorption (Akpomie and Dawodu 2015). In the current study, the value of E was found to be < 8 kJ/mol so the biosorption process was physical in

Table 4 Isotherm parameters for the adsorption of Cr(VI) onto HCSC

Isotherm models	Parameter
Langmuir	
Q_o (mg/g)	231.7
K_L (L/mg)	0.009259
R^2	0.888
X^2	11.2562
Freundlich	
$1/n$	1.098
K_F (mg/g) $(mg/L)^{1/n}$	106.29
R^2	0.9193
X^2	6.6344
Temkin	
A_T (L/ mg)	5.9232
b_T	46.60
B (mg/g)	53.167
R^2	0.878
X^2	6.4262
Dubinin–Radushkevich	
q_s (mg/ g)	128.57
k_{ad} (mol^2/KJ^2)	E−07
E (KJ/ mol)	2.236
R^2	0.9307
X^2	49.9416

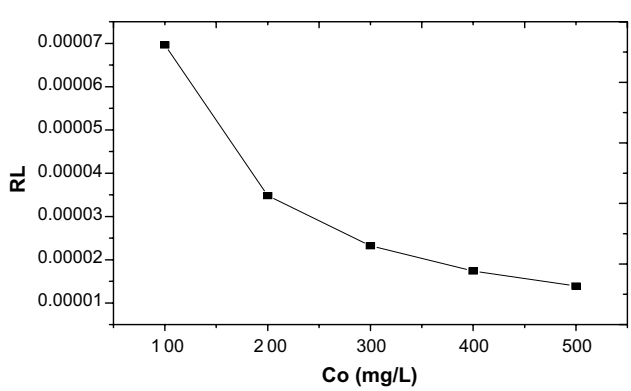

Fig. 9 Separation factor for the adsorption of Cr(VI) onto HCSC powder

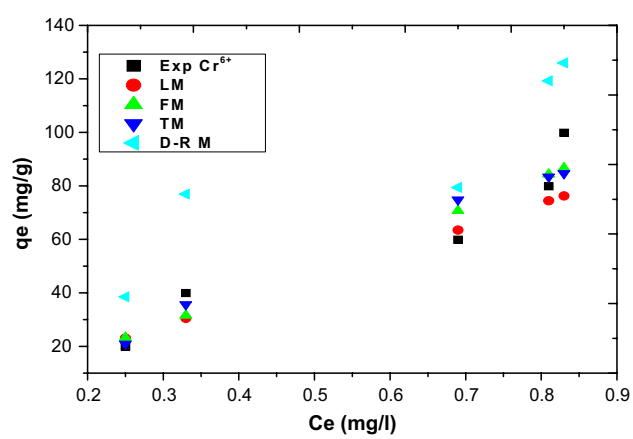

Fig. 10 Comparison of experimental data with the theoretical data for equilibrium isotherm studies for the adsorption of Cr(VI) onto HCSC

nature. Comparison of the isotherm models based on the χ^2 and r^2 values showed a better description of the sorption process by the Freundlich model than Langmuir, Tempkin and Dubinin–Radushkevich isotherm model and the Freundlich model correlated better with the experimental profile in Fig. 10.

Thermodynamic studies

Investigation of thermodynamic study was carried out through study of equilibrium at different temperatures to obtain corresponding values of C_a and C_e. Equilibrium constant, K was obtained from these values and deduced using the relationship

$$K = \frac{C_a}{C_e} \tag{16}$$

K represents the thermodynamic equilibrium constant (Sarin et al. 2006). The following relationship represents the Gibb's free energy ΔG(J/mol):

$$\Delta G = -RTInK \tag{17}$$

The Vant Hoff expression below represents the relationship between the Gibb's free energy, the enthalpy change (ΔH) and entropy change (ΔS) at constant temperature according to thermodynamics:

$$InK = -\left(\frac{\Delta H}{RT}\right) + \left(\frac{\Delta S}{T}\right) \tag{18}$$

The value of ΔG^o,ΔH^o and ΔS^o for the biosorption of Cr(VI) on the HCSC powder is given in Table 5. The positive values of ΔH^o suggests the endothermic nature of the adsorption and the negative values of ΔG^o revealed that the biosorption process was thermodynamically feasible and spontaneous in nature. Similarly, the values of ΔG^o become more negative as the temperature of the metal ions increased, this results indicated that the adsorption process is more favorable at high temperature. The increase in adsorption with increasing temperature indicated endothermic nature of the adsorption process and has been well reported for other adsorbents by other investigators (Prakashan et al. 1999; Arica et al. 2005). The rise in sorption with corresponding rise in temperature may be as a result of either increase in the number of active surface sites available for binding of the metal ions by the adsorbent or due to the increase in the thickness of boundary layer surrounding the sorbent, so the resistance of mass transfer of the adsorbent in the boundary layer is diminished (Meena et al. 2005). Furthermore, the small values of ΔH^o are not in alignment with the formation of strong chemical bonds; hence, it indicates physiosorption process and this corroborated the report of the D–R energy value.

Recovery of sorbent by adsorption–desorption cycle

For the adsorption process to be more viable and practical, it is essential to examine the recovery of the adsorbents via regeneration process by treating the used adsorbent material with a suitable eluent such as HNO_3. Desorption and regeneration data are presented in Table 6. In the present investigation, 0.1 M HNO_3 has been used to examine metal desorption ability from the HCSC powder. Previous investigation by Chojnacka et al. (2005) on desorption of Cd, Cu and Cr from *Spirulina* sp. using 0.1 M EDTA, 0.1 M HNO_3 and deionized water revealed that the most accurate desorbing agent was 0.1 M HNO_3 which eliminated 98% of all the metal ions held unto the biomass as against 0.1 M EDTA efficiency of desorption. In the present study, 0.1 M HNO_3 was used to obtain a percentage desorption of 95.81% Cr(VI) in the first cycle and is therefore good for the adsorbent regeneration. As the number of cycles increased, a gradual decrease in Cr(VI) adsorption was observed as shown in Table 6. Following a sequence of three cycles, the adsorbent uptake capacity for Cr(VI) had been diminished from 94.34 to 80.68%. This decrease may be due to weight loss of the adsorbent during washing and the reduction in the number of actives sites due to the inability of all loaded Cr(VI) ions to be removed. High desorption efficiency of all the three cycles was obtained which was greater than 85% recovery of Cr(VI). The small proportion of sorbed metal that cannot be recovered by regeneration process probably indicates that this portion was strongly bonded, as a result sorption capacity was diminished in the successive cycle. The output validates that HCSC can be utilized repeatedly in the elimination of Cr(VI) ions from polluted medium which is desirable for an efficient biosorbent.

Treatment of textile wastewater using HCSC

To study the effectiveness of HCSC for the elimination of metallic compounds from aqueous phase, it is essential to examine the potential of the biosorbent with industrial wastewater. The result of the characterized textile wastewater obtained from the textile industry located in Lagos state, Nigeria, is presented in Table 7. The wastewater was found

Table 5 Values of thermodynamic parameters for the biosorption of Cr(VI) ions onto HCSC

Metal ion	Temp. (K)	K_D (L g^{-1})	ΔG_o (KJ mol^{-1})	ΔH_o (KJ mol^{-1})	ΔS_o (KJ mol^{-1} K^{-1})	R^2
Cr^{6+}	298	46.28132	−9.50084	0.728445	0.013575	0.3108
	313	45.83841	−9.97907			
	328	51.49344	−10.7483			

Table 6 Adsorption–desorption values for Cr(VI) with 0.1MHNO_3 as the desorbing agent

No. of cycles	Adsorption %	Desorption %
1	94.34	95.81
2	87.15	91.79
3	80.68	88.54

Table 7 Physicochemical parameters of the textile industrial effluent

Constituents	Amounts
pH	3.40
Odor	Objectionable
Color	Yellowish
Total suspended solids (mg/L)	260
Total dissolved solids (mg/L)	135
Total solids (mg/L)	400
Turbidity, NTU	20.7
Cr(VI) (mg/L)	2.28
Cu(II) (mg/L)	2.16
Cd(II) (mg/L)	1.19
Ni(II) (mg/L)	N/A
Pb(II) (mg/L)	0.04
Co(II) (mg/L)	0.0018
BOD (mg/L)	1238
COD (mg/L)	995

to consist of 2.28 mg/L of Cr(VI), which is relatively high. In order to understand the elimination of Cr(VI) from the textile wastewater in the presence of other interfering adsorbates, an array of HCSC dosage between 0.05 and 0.3 g was used. The result is shown in Fig. 11. Effective elimination of

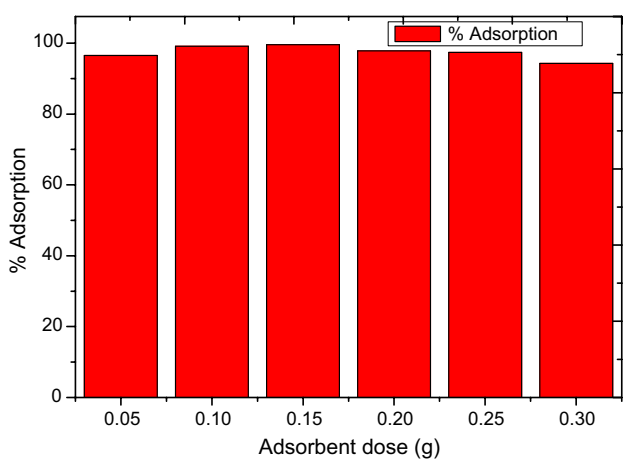

Fig. 11 Effect of adsorbent dose on the removal of Cr(VI) from textile wastewater by HCSC

Cr(VI) ions from the aqueous phase in the presence of other compounds was obtained. When the amount of adsorbent was less than 0.15 g, Cr(VI) adsorption reduced due to the interactions of other ions with the surface of the biomass. This suggests the presence of competitive adsorption taking place between the other contaminants (adsorbate) and HCSC; as a result, there was a reduction in the adsorption of Cr(VI) with smaller amount of HCSC. When the dosage increases correspondingly, the competition decreased as a result of presence of additional active sites and this enhanced Cr(VI) adsorption onto HCSC surface (Anirudhan and Ramachandran 2014). However, the high percentage removal of Cr(VI) from the textile effluent suggested the usefulness of HCSC not only for removal of metal ions from single stock solution but from contaminated effluents in the presence of other pollutants.

Conclusions

This study revealed the use of *H. Crinita* seed coat powder as a biosorbent for removing Cr(VI) ions from textile wastewater and synthetic solution. The biosorbent dosage, pH, contact time, temperature and initial metal ion concentration were found to have significant effect on Cr(VI) biosorption efficiency. The maximum biosorption capacity of powdered *Heinsia crinita* seed coat at optimum pH 2 was 231.7 mg/g. Furthermore, the FT-IR showed several functional groups responsible for biosorption of Cr(VI) on the biosorbent and SEM morphology showed a porous structure. The kinetic studies showed that the biosorption process best fit the pseudo-second-order kinetic model. The equilibrium sorption study showed that Freundlich isotherm model gave the best fit to the experimental data. The calculated thermodynamic parameters revealed the endothermic, spontaneous nature of biosorption and physical adsorption of Cr(VI) ion onto powdered *H. Crinita* seed coat. Desorption and regeneration of the adsorbent for Cr(VI) ion was found to be effective. The biosorbent was suitable for removal of Cr(VI) from contaminated textile wastewater. Thus, it may be concluded that *H. crinita* seed coat powder showed the potential for application in treatment of polluted waters contaminated with Cr(VI) ions. This study was, however, limited to the removal of Cr(VI) ions, further studies could be performed on evaluating the adsorption potential of *H. Crinita* seed coat for other heavy metals as well as organic pollutants.

Compliance with ethical standards

Conflict of interest All authors declare that they have no conflict of interest.

Open Access This article is licensed under a Creative Commons Attribution 4.0 International License, which permits use, sharing, adaptation, distribution and reproduction in any medium or format, as long as you give appropriate credit to the original author(s) and the source, provide a link to the Creative Commons licence, and indicate if changes were made. The images or other third party material in this article are included in the article's Creative Commons licence, unless indicated otherwise in a credit line to the material. If material is not included in the article's Creative Commons licence and your intended use is not permitted by statutory regulation or exceeds the permitted use, you will need to obtain permission directly from the copyright holder. To view a copy of this licence, visit http://creativecommons.org/licenses/by/4.0/.

References

Acharya J, Sahu JN, Sahoo BK, Mohanty CR, Meikap BC (2009) Removal of chromium(VI) from wastewater by activated carbon developed from tamarind wood activated with zinc chloride. Chem Eng J 150(1):25–39

Ahmad A, Ghazi ZA, Saeed M, Llyas M, Ahmad R, Khattak AM, Iqbal A (2017) Comparative study of the removal of Cr(VI) from synthetic solution using natural biosorbents. New J Chem 41:10799

Akinfolarin OM, Gbarakoro SL (2016) Proximate analyses of Atama (*Heinsia crinita*) and Editan (*Lasianthera africans*) in a packed bed: comparison with granular activated carbon. Process Biochem 38:175–186

Akpomie KG, Dawodu FA (2015) Physicochemical analysis of automobile effluent before and after treatment with an alkaline activated montmorillonite. J Taibah Univ Sci 9:465–476

Akpomie KG, Onyeabor CF, Ezeofor CC, Ani JU, Eze SI (2019) Natural aluminosilicate clay obtained from south Eastern Nigeria as potential sorbent for oil spill remediation. J Afr Earth Sci 155:118–123

Aksu Z, Gonen F, Demircan Z (2002) Biosorption of chromium(VI) ions by mowital B30H resin immobilized activated sludge. IOSR J Appl Chem 9(3):76–79

Al-Othman ZA, Ali R, Naushad M (2012) Hexavalent chromium removal from aqueous medium by activated carbon prepared from peanut shell: adsorption kinetics, equilibrium and thermodynamic studies. Chem Eng J 184:238–247

American Public Health Association (APHA) (2005) Standard methods for the examination of water and wastewater, 20th edn. APHA, Washington DC

Anandkumar J, Mandal B (2009) Removal of Cr(VI) from aqueous solution using Bael fruit (*Aeglemarme loscorrea*) shell as an adsorbent. J Hazard Mater 168:633–640

Ani JU, Ochonogor AE, Akpomie KG, Olikagu CS, Igboanugo CC (2019) Abstraction of Arsenic(III) on activated carbon prepared from dialium guineense seed shell: kinetics isotherms and thermodynamic studies. SN Appl Sci 1:1304

Anirudhan TS, Ramachandran M (2014) Removal of 2, 4, 6-trichlorophenol from water and petroleum refinery industry effluents by surfactant-modified bentonite. J Water Process Eng 1:46–53

Anjana K, Anubha K, Kiran B, Nisha R (2007) Biosorption of Cr(VI) by immobilized biomass of two indigenous strains of cyanobacteria isolated from metal contaminated soil. J Hazard Mater 148:383–386

Arica MY, Tüzün I, Yalçin E, Ince Ö, Bayramoglu G (2005) Utilization of native, heat and acid-treated microalgae preparations for biosorption of Cr(VI) ions. Process Biochem 40:2351–2358

Asuquo E, Martin A, Nzerem P, Siperstein F, Fan X (2017) Adsorption of Cd(II) and Pb(II) ions from aqueous solutions using mesoporous activated carbon adsorbent: equilibrium, kinetics and characterisation studies. Biochem Pharmacol 5(1):679–698

Cardoso NF, Pinto RB, Lima EC, CalveteT Amavisca CV, Royer B, Cunha ML, Fernandes THM, Pinto IS (2011) Removal of remazol black B textile dye from aqueous solution by adsorption. Desalination 269:92–103

Chojnacka K, Chojnacki A, Gorecka H (2005) Biosorption of Cr^{3+}, Cd^{2+} and Cu^{2+} ions by blue–green algae *Spirulina* sp.: kinetics, equilibrium and the mechanism of the process. Chemosphere 59:75–84

Chukwuemeka-Okorie HO, Ekemezie PN, Akpomie KG, Olikagu CS (2018) Calcined concob-kaolinite combo as new sorbent for sequestration of toxic metal ions from polluted aqua media and desorption. Front Chem 6:1–13

Dakiky M, Khamis M, Manassra A, Mer'eb M (2002) Selective adsorption of Cr(VI) in industrial wastewater using low cost abundantly available adsorbents. J Adv Environ Res 6:533–540

Dang VBH, Doan HD, Dang-vu T, Lohi A (2009) Equilibrium and kinetics of biosorption of cadmium(II) and copper(II) ions by wheat straw. Biores Technol 100:211–219

Dawodu FA, Akpomie KG (2014) Simultaneous adsorption of Ni(II) and Mn(II) ions from aqueous solution unto a Nigerian kaolinite clay. J Mater Res Technol 3(2):128–141

Dawodu FA, Onuh CU, Akpomie KG, Unuabonah EI (2019) Synthesis of silver nanoparticle from *vigna unguiculata* stem as adsorbent for malachite green in a batch system. SN Appl Sci 1:346

Dubinin MM (1960) The potential theory of adsorption of gases and vapors for adsorbents with energetically non-uniform surface. Chem Rev 60:235–266

EPA (Environmental Protection Agency), Environmental Pollution Control Alternatives, 1990, EPA/625/5-90/025, EPA/625/4-89/023, Cincinnati, US

Etukudo I (2003) Ethnobatany: conventional and traditional use of plants. Verdict Press, Uyo, Nigeria

Eze SI, Akpomie KG, Ezeofor CC, Osunkunle AA, Maduekwe OB, Okenyeka OU (2019) Isotherm and kinetic evaluation of *Dialium guineense* seed husk and its modified derivatives as efficient sorbent for crude oil polluted water treatment. Water Conserv Sci Eng. https://doi.org/10.1007/s41101-019-00065-6

FEPA (1991) Guidelines and standards for environmental pollution control in Nigeria. Federal Environmental Protection Agency FEPA, Lagos

Gunay A, Arslankaya E, Tosun I (2007) Lead removal from aqueous solution by natural and pretreated clinoptilolite: adsorption equilibrium and kinetics. J Hazard Mater 146:362–371

Hall KR, Eagleton LC, Axerivos A, Vermeuleu T (1966) Pore and solid diffusion kinetics in fixed bed adsorption under constant pattern conditions. Ind Eng Chem Fundam 5:212–216

Ho YS, Mckay G (1998) The kinetics of sorption of basic dyes from aqueous solution by *Sphagnum moss peat*. Can J Chem Eng 76:822–827

Ibigbami T, Dawodu F, John O (2016) Removal of heavy metals from pharmaceutical industrial wastewater effluent by combination of adsorption and chemical precipitation methods. Am J Appl Chem 4(1):24–32

Kabata-Pendias A (2001) Trace elements in soils and plants, 3rd ed., A. Kabata Pendias and H. Pendiaseds., CRC, Boca Raton

Kamsonlian S, Suresh S, Majumder CB, Chand S (2012) Biosorption of arsenic from contaminated water onto solid *Psidiumguajava* leaf surface: equilibrium, kinetics, thermodynamics and desorption study. Bioremediat J 16(2):97–112

Karimi M, Shojaei A, Nematollahzadeh A, Abdekhodaie MJ (2012) Column study of Cr(VI) adsorption onto modified silica–polyacrylamide microspheres composite. Chem Eng J 210:280–288

Kiran B, Kaushik A, Kaushik CP (2007) Biosorption of Cr(VI) by native isolate of *Lyngbyaputealis* (HH-15) in the presence of salts. J Hazard Mater 141:662–667

Kumar PS, Ramakrishnan K, Kirupha DS, Sivanesan S (2010) Thermodynamic and kinetic studies of cadmium adsorption from aqueous solution onto rice husk. Braz J Chem Eng 27(2):437–455

Langmuir I (1918) The adsorption of gases on plane surfaces of glass, mica and platinum. J Am Chem Soc 40:1361–1403

Lazaridis NK, Asouhidou DD (2003) Kinetics of sorptive removal of chromium (VI) from aqueous solutions by calcined Mg–Al–CO_3hydrotalcite. Water Res 37:2875–2882

Li J, Qi T, Wang L, Liu C, Zhang Y (2007) Synthesis and characterization of imidazole- functionalized SBA-15 as an adsorbent of hexavalent chromium. Mater Lett 61:3197–3200

Li WX, Gong X, Li D, Zhang H, Gong H (2012) Removal of Cr(VI) from low-temperature micro- polluted surface water by tannic acid immobilized powdered activated carbon. Biores Technol 113:106–113

Mclaughlin MJ, Zarcinas BA, Stevens DP, Cook N (2000) Soil testing for heavy metals. Commun Soil Sci Plant Anal 31:1661–1700

Meena AK, Mishra GK, Rai PK, Rajagopal C, Nagar PN (2005) Removal of heavy metal ions from aqueous solutions using carbon aerogel as an adsorbent. J Hazard Mater 122:161–170

Melo JS, Souza SFD (2004) Removal of chromium by mucilaginous seeds of *Ocimum basilicum*. Bioresour Technol 92:151–155

Nadeem R, Asif M, Mahmood A, Salman M, Ashraf M (2009) Biosorption of Cu(II) ions from aqueous effluents by blackgram bran (BGB). J Hazard Mater 168:1622–1625

Njoya A, Nkoumbou C, Grosbois C, Njopwouo D, Njoya D, Courtin-Nkoumbou A (2006) Genesis of mayouom kaolin deposit (western Cameroun). Appl Clay Sci 32:125–140

Okokon JE, Anita BS, Umoh EE (2009) Antiulcerogenic activity of ethanolic leaf extract of *Lasianthera africana*. Afr J Tradcompl 6:150–154

Ouyang X, Yang L, Wen Z (2014) Adsorption of Pb(II) from solution using peanut shell as biosorbent in the presence of amino acid and sodium chloride. BioResources 9(2):2446–2458

Ozdemir G, Ceyhan N, Ozturk T, Akirmak F, Cosar T (2004) Biosorption of chromium(VI), cadmium(II) and copper(II) by *Pantoea* sp. TEM18. Chem Eng J 102:249–253

Padmesh TVN, Vijayaraghavan K, Sekaran G, Velan M (2006) Biosorption of acid blue 15 using fresh water macroalga *azolla filiculoides*: batch and column studies. Dyes Pigm 71:77–82

Pakade VE, Ntuli TD, Ofomaja AE (2017) Biosorption of hexavalent chromium from aqueous solutions by Macadamia nutshell powder. Appl Water Sci 7:3015–3030

Parlayici S, Pehlivan E (2019) Comparative study of Cr(VI) removal by bio-waste adsorbents: equilibrium kinetics and thermodynamics. J Anal Sci Technol. https://doi.org/10.1186/s40543-019-0173-3

Prahas D, Kartika Y, Indraswati N, Ismadji S (2008) Activated carbon from jackfruit peel waste by H_3PO_4 chemical activation: pore structure and surface chemistry characterization. Chem Eng J 140:32–42

Prakashan RS, Merrie JS, Sheela R, Saswathi N, Ramakrishna SV (1999) Biosorption of chromium(VI) by free and immobilized *Rhizopu sarrhizus*. Environ Pollut 104:421–427

Rafatullah M, Sulaiman O, Hashim R, Ahmad A (2009) Adsorption of copper(II), chromium(III), nickel(II) and lead(II) ions from aqueous solutions by meranti sawdust. J Hazard Mater 170:969–977

Rangabhashiyam S, Selvaraju N (2014) Evaluation of the biosorption potential of a novel *Caryotaurens* inflorescence waste biomass for the removal of hexavalent chromium from aqueous solutions. J Taiwan Inst Chem Eng 51:10–19

Saer GW (1956) Determination of Specific surface area of sodium hydroxide. Anal Chem 28(2):1981–1983

Samani MR, Borghei SM, Olad A, Chaichi MJ (2010) Removal of chromium from aqueous solution using polyaniline-poly ethylene glycol composite. J Hazard Mater 184:248–254

Sarin V, Singh TS, Pant KK (2006) Thermodynamic and breakthrough column studies for the selective sorption of chromium from industrial effluent on activated eucalyptus bark. Biores Technol 97:1986–1993

Skoog DA, Holler FJ, Nieman TA (1998) Principles of Instrumental Analysis, 5th edn. Sounders College Publisher, Philadelphia

Sridhara N, Kamala C, Samuel D (2008) Assessing risk of heavy metals from consuming food grown on sewage irrigated soils and food chain transfer. Ecotoxicol Environ Saf 3:513–524

Tempkin MI, Pyzhev V (1940) Kinetics of ammonia synthesis on promoted iron catalyst. Acta Phys Chim USSR 12:327–356

Tsia WT, Chen HR (2010) Removal of malachite green from aqueous solution using low-cost chlorella based biomass. J Hazard Mater 175(1–3):844–849

Ucun H, Bayhan YK, Kaya Y, Cakici A, Algur OF (2002) Biosorption of chromium(VI) from aqueous solution by cone biomass of *Pinussylvestris*. Biores Technol 85:155–158

Vaghetti JCP, Lima EC, Royer B, Brasil JL, Bruna M, Simon NM, Cardoso NF, Zapata CP (2008) Application of Brazilian-pine fruit coat as a biosorbent to removal of Cr(VI) from aqueous solution: kinetics and equilibrium study. Biochem Eng J 42:67–76

Viswanathan N, Sundaram CS, Meenakshi S (2009) Sorption behaviour of fluoride on carboxylated cross-linked chitosan beads. Colloids Surf B Biointerfaces 68:48–54

Webber TN, Chakravarti RK (1974) Pore and solid diffusion model for fixed bed adsorbers. Am Inst Chem Eng 20:228–238

Weber WJ, Morris JC (1963) Kinetics of adsorption on carbon from solution. J Sanit Eng Div Am Soc Civil Eng 89:31–60

Yargic AS, Yarbay-Sahin RZ, Ozbay N, Onal E (2014) Assessment of toxic copper(II) biosorption from aqueous solution by chemically-treated tomato waste (*Solanumly copersicum*). J Clean Prod 79:1–8

Yusuff AS (2019) Adsorption of hexavalent chromium from aqueous solution by *Leucaena leucocephala* seed pod activated carbon: equilibrium kinetic and thermodynamic studies. Arab J Basic Appl Sci 26:89–102

Zahra A, Mohammad A, Eshagh RN, Farzaneh M, Vahid M (2013) Adsorptive removal of Co^{2+} and Ni^{2+} by peels of banana from aqueous solution. Univ J Chem 1(3):90–95

Publisher's Note Springer Nature remains neutral with regard to jurisdictional claims in published maps and institutional affiliations.